Finite Volume Method Applied to Symmetrical Structures in Coupled Problems

Ioana - Gabriela Sîrbu

University of Craiova, Electrical Engineering Faculty, Decebal Blv. No. 107, 200440-Craiova, Romania osirbu@elth.ucv.ro

This paper presents a possibility of modelling the electromagnetic field, by taking into account the symmetry of the domains. The domain discretisation and implicitly the finite volume shape will be derived from the type of the symmetry. Thus, a reduction of the problem size, as well as a guaranteed symmetry of the solution, and a better approximation of the borders and of the discontinuity surfaces are achieved.

1 Introduction

Cell complexes are basic tools of algebraic topology. A cell complex can be based on a coordinate system; in such a case the edges of the cells lie on the coordinate lines and the faces on the coordinate surfaces. The advantages of these complexes are the easy utilization, the amount of memory may be not too high and they are used to develop fast algorithms that are adapted to the vectorial architecture. Their limitations come from the domain borders and from the object discretisation, where special treatments are necessary, the main problem being the approximation of the solution near the borders and in the interface zones.

For numerical applications one prefers to drop out these cell complexes based on coordinates and to use non-structured cells of triangular or tetrahedral finite element type. These cells can easily be adapted to any complex geometry. Moreover finite element method was developed in great detail, the problem of the domain discretisation in triangular or tetrahedral cells being already solved. Almost all the software instruments for field modelling use the discretisation of triangular finite element type. These cell complexes have advantages on those that are based on coordinates: (1) the simplified cells can easily be adapted to the domain border; (2) can include regions of different materials; (3) the points can be taken on the separation surface; (4) the cells can have different dimensions in one zone or another. In order to model the electromagnetic field two cells complexes will be considered in this work: the Delaunay complex (primal complex) and associated Voronoi complex (dual complex) [Ton01].

In literature, the orthogonal grids were not completely abandoned. Some researchers try to find out solutions in order to eliminate the inconveniences of the method, for example by introducing a new consistent subgridding method, which allows an increased flexibility of mesh configurations with local refinement [PCW03].

This paper tries to find out a possibility of modelling the electromagnetic field in the symmetrical structures case, using curvilinear grids. This solution, even if it is not applicable to general problems, aims to simplify the problem size and to eliminate inconveniences near specific borders.

2 Symmetrical Structures Modelling

2.1 Electromagnetic Field Modelling

In rotationally symmetric structures, generation and adaptation of the grid may involve primal and dual cell complexes, as shown in Fig. 1.

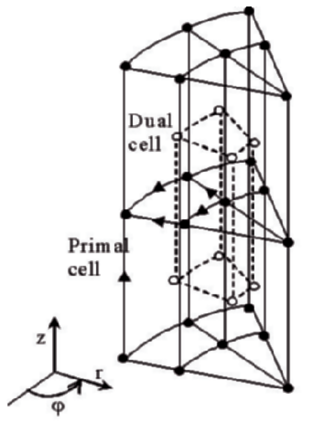

Fig. 1: Cells of the primal and dual complexes

A Yee-type scheme was chosen; every element (volume) of a cell complex includes a point of the other (dual) cell complex. Thus every surface of a grid will be intersected by a single line of the other grid. One associates the components of the electric field vector to the lines of the primal grid and the components of the magnetic field vector to the lines of the dual grid.
In order to model the electromagnetic field, the Maxwell's equations will be used:

$$\oint_{\Gamma} \overline{E} \cdot \overline{dr} = -\frac{d}{dt} \int_{S_\Gamma} \overline{B} \cdot \overline{dS} \tag{1}$$

$$\oint_{\Gamma} \overline{H} \cdot \overline{dr} = i_{S_\Gamma} + \frac{d}{dt} \int_{S_\Gamma} \overline{D} \cdot \overline{dS}$$

$$\oint_{\Sigma} \overline{D} \cdot \overline{dS} = q_\Sigma$$

$$\oint_{\Sigma} \overline{B} \cdot \overline{dS} = 0$$

where E, B, H and D are the electric field strength, the magnetic induction, the magnetic field strength and the electric induction respectively; q_Σ is the electric charge

inside Σ and i_{S_Γ} is the current through the surface delimited by Γ. These equations are completed by the constitutive equations.
With the notations:l- a line of the primal grid that belongs to the face f of this grid, $\widetilde{l}$- the face of the dual grid crossed by the line l and $\widetilde{f}$ - the line of the dual grid that crosses the face f, the first two relations of Maxwell's equations (1), applied to cells of the primal grid and of the dual grid respectively, becomes:

$$-\frac{\partial \varphi_f}{\partial t} = \sum_{l\in\partial f} \pm u_{el} \tag{2}$$
$$\frac{\partial \psi_{\widetilde{l}}}{\partial t} + i_{\widetilde{l}} = \sum_{\widetilde{f}\in\partial\widetilde{l}} \pm u_{m\widetilde{f}}$$

where φ_f is the magnetic flux through the face f, u_{el} is the electric voltage corresponding to the line l, $\psi_{\widetilde{l}}$ is the electric flux through the face $\widetilde{l}$ and $u_{m\widetilde{f}}$ is the magnetic voltage corresponding to the line $\widetilde{f}$; ∂f is the border of the face f and $\partial\widetilde{l}$ is the border of the face $\widetilde{l}$; the sign is "+" if the sign of the line l ($\widetilde{f}$) is associated to the sense of the face f ($\widetilde{l}$) by the rule "of the screw" and "-" if it is opposite.
Considering that on every face and on every line the electric or magnetic field value is constant and choosing as unknowns the magnetic fluxes and the electric voltages (corresponding to the primal grid), the system (2) becomes:

$$-\frac{\partial \varphi_f}{\partial t} = \sum_{l\in\partial f} \pm u_{el} \tag{3}$$
$$\frac{\partial}{\partial t}(\varepsilon \frac{A_{\widetilde{l}}}{L_l} u_{el}) + \sigma \frac{A_{\widetilde{l}}}{L_l} u_{el} = \sum_{\widetilde{f}\in\partial\widetilde{l}} (\pm\frac{1}{\mu} \cdot \frac{L_{\widetilde{f}}}{A_f} \cdot \varphi_f)$$

where ε is the permittivity of the medium, σ is the electrical conductivity, μ is the permeability; A_f ($A_{\widetilde{l}}$) is the area of the face f ($\widetilde{l}$) and L_l ($L_{\widetilde{f}}$) is the length of the line l ($\widetilde{f}$).
If the field variables do not depend on the z-coordinate and the domain has a cylindrical geometry, the problem is reduced to a 2-dimensional case (see Fig.2). In this case the first equation of (3) remains identical, while the second one is written as:

$$\frac{\partial}{\partial t}(\varepsilon \frac{\Delta r}{l_{arc}} u_{el}) + \sigma \frac{\Delta r}{l_{arc}} u_{el} = \sum_{\widetilde{f}\in\partial\widetilde{l}} (\pm\frac{1}{\mu} \cdot \frac{1}{A_{sector}} \cdot \varphi_f) \tag{4}$$

or

$$\frac{\partial}{\partial t}(\varepsilon \frac{l_{arc}}{\Delta_r} u_{el}) + \sigma \frac{l_{arc}}{\Delta r} u_{el} = \sum_{\widetilde{f}\in\partial\widetilde{l}} (\pm\frac{1}{\mu} \cdot \frac{1}{A_{sector}} \cdot \varphi_f) \tag{5}$$

in accordance to the line type that was considered (a part of an arc or of a radius).
For temporal discretisation the FDTD method was chosen.

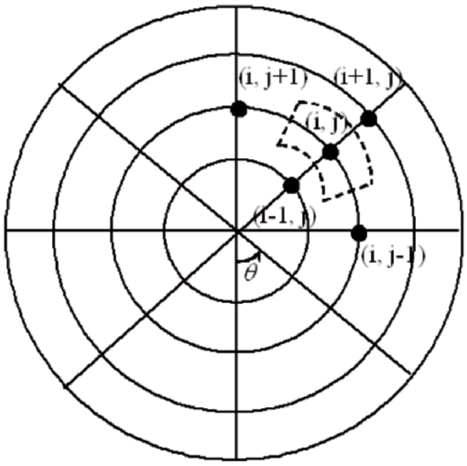

Fig. 2: Cylindrical symmetry structure - 2-dimensional case

2.2 Thermal Field Modelling

If the thermal field modelling is also wanted, the primal grid will be used. Thus coupled problems can be solved [MEU02].
The thermal conduction equation in a variable regime is considered. In a cylindrical symmetry case, one finds [POP02]:

$$\rho c_p \frac{\partial T}{\partial t} = \frac{1}{r} \cdot \frac{\partial}{\partial r}(r\lambda \frac{\partial T}{\partial r}) + \frac{1}{r^2} \cdot \frac{\partial}{\partial \theta}(\lambda \frac{\partial T}{\partial \theta}) + \frac{\partial}{\partial z}(\lambda \frac{\partial T}{\partial z}) + S \tag{6}$$

where ρ is the material density, c_p is the specific heat, T is the temperature, λ is the thermal conductivity and S is the power generated in a volume unit (function of electromagnetic field).
In the 2-dimensional case, if the field distribution in the section is not symmetrical, this equation becomes:

$$\rho c_p \frac{\partial T}{\partial t} = \frac{1}{r} \cdot \frac{\partial}{\partial r}(r\lambda \frac{\partial T}{\partial r}) + \frac{1}{r^2} \cdot \frac{\partial}{\partial \theta}(\lambda \frac{\partial T}{\partial \theta}) + S \tag{7}$$

For the primal grid represented in the Fig. 2, where the angle θ can be considered having the same value for all the sectors, this relation, integrated on a control volume built around a point (i,j) of the grid, becomes:

$$\begin{aligned} \int_t^{t+\Delta t} \int_{VC} \rho c_p \frac{\partial T}{\partial t} dV dt = \int_t^{t+\Delta t} \int_{VC} \frac{1}{r} \cdot \frac{\partial}{\partial r}(r\lambda \frac{\partial T}{\partial r}) dV dt + \\ + \int_t^{t+\Delta t} \int_{VC} \frac{1}{r^2} \cdot \frac{\partial}{\partial \theta}(\lambda \frac{\partial T}{\partial \theta}) dV dt + \int_t^{t+\Delta t} \int_{VC} S dV dt \end{aligned} \tag{8}$$

where $dV = d\theta \cdot r \cdot dr \cdot 1$.
Applying Euler-backward time integration to (8), the following relation is obtained:

$$\rho c_p \theta (T_{i,j} - T_{i,j}^0) \cdot r_i \cdot \Delta r = r_{i+\frac{1}{2}} \cdot \lambda_{i+\frac{1}{2}} \cdot \theta \cdot \Delta t \frac{T_{i+1,j} - T_{i,j}}{\Delta r_i} - \tag{9}$$

$$- r_{i-\frac{1}{2}} \cdot \lambda_{i-\frac{1}{2}} \cdot \theta \cdot \Delta t \frac{T_{i,j} - T_{i-1,j}}{\Delta r_{i-1}} + \lambda_{j+\frac{1}{2}} \frac{2 r_i \Delta r \Delta t}{r_{i-\frac{1}{2}}^2 \cdot r_{i+\frac{1}{2}}^2} \cdot \frac{T_{i,j+1} - T_{i,j}}{\Delta \theta} -$$

$$- \lambda_{j-\frac{1}{2}} \frac{2 r_i \Delta r \Delta t}{r_{i-\frac{1}{2}}^2 \cdot r_{i+\frac{1}{2}}^2} \cdot \frac{T_{i,j} - T_{i,j-1}}{\Delta \theta} + S \cdot \theta \cdot \Delta r \cdot r_i \cdot \Delta t$$

where $T_{i+k,j+l}$ for $k = -1, 0, 1$, $l = -1, 0, 1$ are the (unknown) temperatures at the gridpoints at the current time level and $T_{i+k,j+l}^0$ is the (known) temperatures at the gridpoints at the previous time level.

2.3 Application

For the validation of the analysed discretisation technique, a numerical application was considered. The simple case of the conductor of copper, placed in air was studied, with radius a = 0.02 m. The r.m.s. value of the current through this conductor is I=200A. Two different frequencies are analysed: f = 50 Hz and 500 Hz.
A MATLAB program was developed for modelling both the electromagnetic field and the thermal field. The modelling results, obtained for the steady-state case, are presented in figures 3-8.

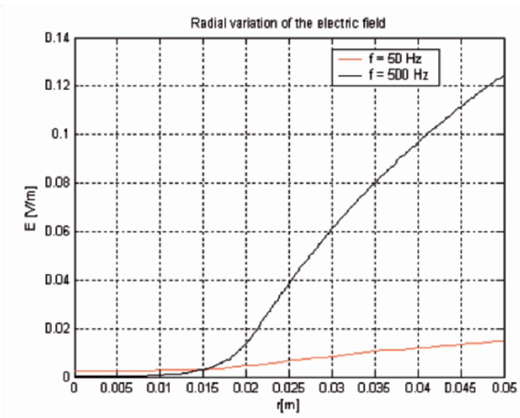

Fig. 3: The radial variation of the electric field

In figures 3 and 4 the electric field and the magnetic field are shown, for the two frequencies, in a comparative manner. Different types of radial variations in conductor and in air were observed. While the electric field increases from the conductor-air border to the domain border, the magnetic field maximum was obtained at the conductor-air border, having the same maximum value for the both values of the frequency.
In figures 5 and 6 the electrical and magnetic fields are presented as functions of r. In both cases f = 500 Hz was taken. We observe that near the z-axis both fields have

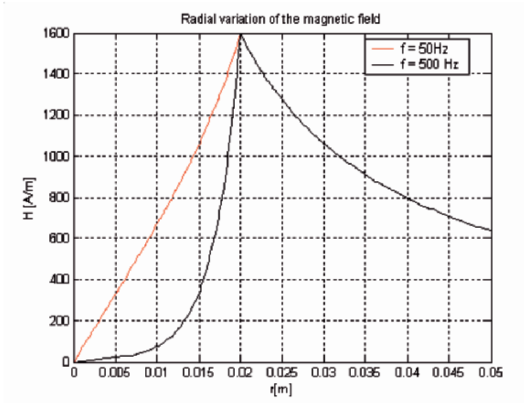

Fig. 4: The radial variation of the magnetic field

a different orientation when compared to the fields further away. This is a result of the high level of the frequency in the conductive medium.

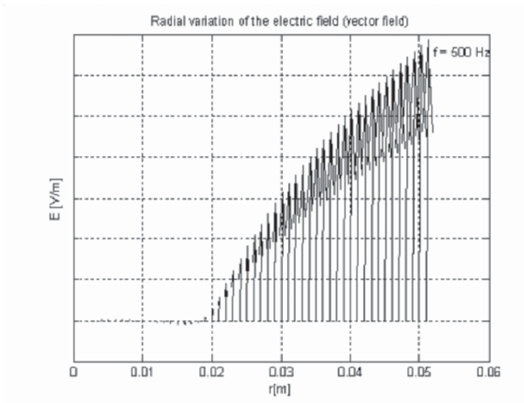

Fig. 5: The radial variation of the electric field (the vector field, for f = 500 Hz)

As for the thermal field, it was shown in figures 7 and 8 only for the conductive medium, for the same frequencies. A forced air cooling was considered. The boundary condition was of convection type. Because of the thinness of the conductor and of the cooling type that it was chosen, the variation of the temperature in the conductor resulted, in this case, very small.
Because of the symmetry of the resulted distributions, only the radial variations of the electric field, of the magnetic field and of the thermal field were represented here.

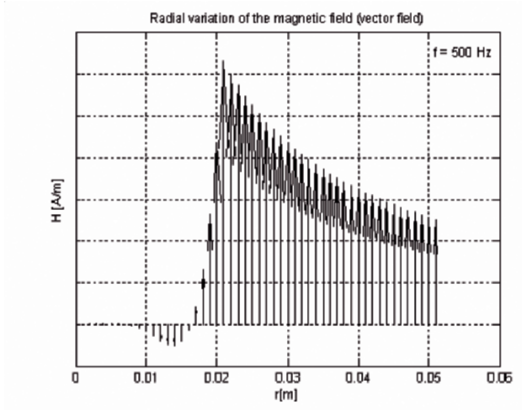

Fig. 6: The radial variation of the magnetic field (the vector field, for f = 500 Hz)

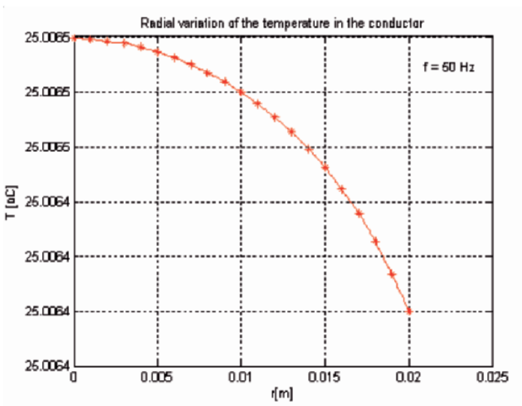

Fig. 7: The radial variation of the temperature for f =50 Hz

These results correspond to the electromagnetic field theory [MOC91]and to the thermal field theory [POP02] and they are similar to those obtained and published by the researchers.
The results were verified by using a dedicated software based on the discretisation of triangular finite element type (Quickfield). The Quickfield software cannot be used for coupled problems, but, using simplifications to accommodate for the couplings, results can be obtained that are approximative to those obtained by our MATLAB program.

3 Conclusion

The paper deals with the specific features of the electromagnetic - thermal coupled modelling in the particular case of the symmetrical distributions. This alternative method aims to increase the accuracy of the solution and to decrease the geometrical

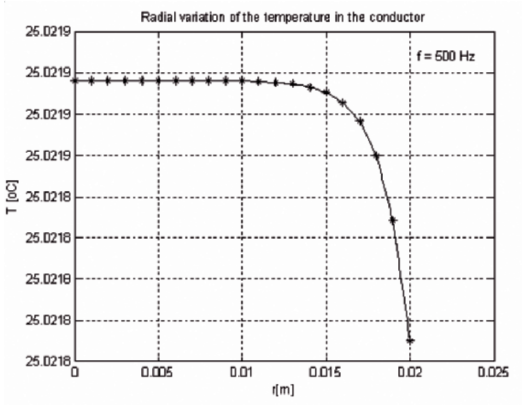

Fig. 8: The radial variation of the temperature for f =500Hz

complexity of the problem when compared to the case when the cartesian coordinates are used. This approach is an alternative to the discretisation of triangular finite element type.

References

[Ton01] Tonti, E.: Finite Formulation Of The Electromagnetic Field. In: Geometric methods for computational electromagnetics (ed) PIER Ser. vol 32 , 1– 44 (2001)

[PCW03] Poděbrad, O., Clemens, M., Weiland, T.: New Flexible Subgridding Scheme for the Finite Integration Technique. In: IEEE Transactions on Magnetics, **39**, no.3, may 2003, 1662–1665 (2003)

[MEU02] Meunier, G.: Electromagnétisme et problèmes couplés, vol.3. Hermes Science Publications, Paris (2002)

[POP02] Popa, I.C.: Modélisation numérique du transfert thermique - Méthode des volumes finis. Ed. Universitaria, Craiova (2002)

[MOC91] Mocanu, C.I.: Bazele electrotehnicii - Teoria câmpului electromagnetic. Ed. Didactică şi Pedagogică, Bucureşti (1991)

[GF03] Ghinea, M., Fireţeanu, V.: MATLAB - Calcul numeric. Grafică. Aplicaţii. Ed. Teora, Bucureşti (2003)

[***] ***: QuickField - User's Guide